Multiple Connected Optical Hard Limiter and Optical Power Equalizer Using Quantum-Dot Semiconductor

Keiichi Iwamoto, Fumiya Sato, Yuma Furuya, Takanori Irie, Gou Hosoya, and Hiroyuki Yashima

Tokyo University of Science, 1-3 Kagurazaka Shinjyuku-ku Tokyo 162-8601 Japan
Email: iwamoto@ms.kagu.tus.ac.jp

Abstract–We propose an optical hard limiter (OHL) and optical power equalizer (OPE) consisting of multiple serially connected OHLs and OPEs. OHL and OPE use quantum-dot semiconductor optical amplifiers (QD-SOAs) based on the nonlinear effect of a self-phase modulation (SPM). By using QD-SOAs to adjust the phase between both arms of a Mach-Zehnder interferometer (MZI), performance of OHL and OPE can be implemented. We numerically analyze the proposed OHL and OPE models, and show that, with respect to previous implementations, the operating range is expanded and the input-output characteristics are improved.

1. Introduction

In the optical communication network, due to the effects of dispersion in the optical fiber and the noise in the amplifier, an optical signal intensity fluctuation occurs, and the power of the optical signal in each bit is not constant. Because of intensity fluctuations, the performance of various optical signal processing techniques may be degraded [1]. Therefore, it is necessary to compensate for the intensity fluctuations.

An optical hard limiter (OHL) can remove the noise generated in the transmission process, and an optical power equalizer (OPE) can align the power of each signal to a constant value. In recent years, studies of OHL and OPE using quantum-dot semiconductor optical amplifiers (QD-SOAs) have been reported [2]. However, the conventional OHL and OPE have the problem that the operating range in which the OHLs and OPEs function is small, and the input-output characteristics are quite different from the ideal characteristics.

In this paper, we propose OHL and OPE consisting of multiple serially connected OHLs and OPEs. The proposed OHL consists of multiple serially connected OHLs, also the proposed OPE consists of multiple serially connected OPEs. We numerically analyze the proposed OHL and OPE models, and show input-output waveforms and the characteristics of the proposed OHL and OPE. The results indicate that, with respect to previous implementations, the operating range of the proposed OHL and OPE are expanded and the input-output characteristics are improved.

This paper is organized as follows. Section 2 describes the working principle of OHL and OPE. In section 3, we present the principle of the proposed OHL and OPE, which use QD-SOAs. In section 4, we describe a theoretical model for OHL and OPE. Section 5 give the results and discusses them, and section 6 is the conclusion.

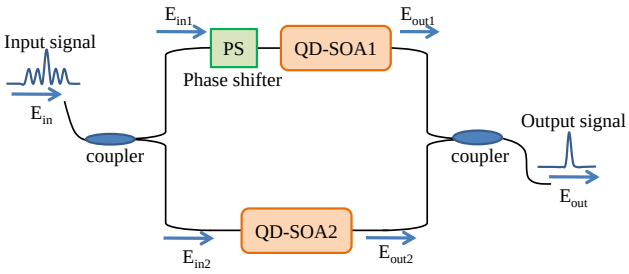

Fig. 1 Schematic diagram of the OHL and OPE.

2. Working Principle of OHL and OPE

A schematic diagram of the OHL and OPE model is shown in Fig. 1 [2]. This model consists of two 3dB couplers, a phase shifter (PS), and two QD-SOAs in a Mach-Zehnder interferometer (MZI) structure. The PS is used to adjust the phase of the signal. The two QD-SOAs operate with the same parameters, except for the maximum gain and the linewidth enhancement factor. The input signal E_{in} is fed into the first coupler and then the signal is split into E_{in1} and E_{in2}. After adjusting the phase by using the PS, E_{in1} passes through QD-SOA1 and is translated into E_{out1}. E_{in2} has an additional 90° phase added by the first coupler and passes through QD-SOA2 to be translated into E_{out2}. Finally, E_{in1} and E_{in2} are recombined by the second coupler to form the output signal E_{out}. By adjusting the PS and maximum gain of QD-SOA, the operation of the OHL or OPE can be realized.

3. Proposed OHL and OPE

In a conventional OHL [2], the input signal power over a threshold is amplified, whereas the signal power under the threshold is attenuated. However, the input-output characteristic is quite different from the ideal one. To obtain the characteristic close to ideal, it is necessary to further discriminate the signal at the threshold. In this paper, we propose an OHL that delivers improved input output characteristics by multiple serially connected OHLs. This allows the output signal power to be further discriminated by passing through multiple OHLs.

In a conventional OPE [2], the output signal is adjusted according to the input signal power to keep the output signal power constant. However, the operating range is insufficient when used in an OPE. In this paper, we propose an OPE that delivers increased operating range by multiple serially connected OPEs. In order to obtain characteristics close to ideal, the output signal power should be kept constant for arbitrary input signal powers. Therefore, by passing through multiple OPEs, we can obtain the improved characteristics.

A schematic of the proposed model is shown in Fig. 2. First, an input signal is fed into the first OHL or OPE. An attenuator (ATT) serves to adjust the output signal to fall within the operating range of the second OHL or OPE. Thereafter, the signal is fed into the second OHL or OPE. By adjusting the output signal power, it is possible to operate the second OHL and OPE, and improve their performance.

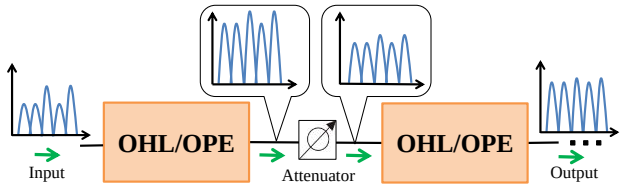

Fig. 2 Proposed OHL and OPE device.

4. Theoretical Model of OHL and OPE

The performance of the QD-SOA is described by a three level rate equation model [3] – [5], which contains a ground state energy model (GS), an excited state (ES) and a wetting layer (WL). The rate equations for carriers in the WL, ES and GS are as follows:

$$\frac{\partial N_w}{\partial t} = \frac{I}{qV} - \frac{N_w(1-h)}{\tau_{w2}} + \frac{N_Q \times h}{\tau_{2w}} - \frac{N_w}{\tau_{wR}} \quad (1)$$

$$\frac{\partial N_Q h}{\partial t} = \frac{N_w(1-h)}{\tau_{w2}} - \frac{N_Q h}{\tau_{2w}} - \frac{N_Q h(1-f)}{\tau_{21}} + \frac{N_Q f(1-h)}{\tau_{12}} \quad (2)$$

$$\frac{\partial N_Q f}{\partial t} = \frac{N_Q h(1-f)}{\tau_{21}} - \frac{N_Q f(1-h)}{\tau_{12}} - \frac{N_Q f^2}{\tau_{1R}} - \frac{g}{\sigma E} P \quad (3)$$

where N_W is the electron density in the WL, I is the injection current, q is the electron charge, V is the volume of the QD-SOA, τ_{w2} is the electron relaxation time from the WL to the ES, τ_{2w} is the electron escape time from the ES to the WL, τ_{wR} is the spontaneous radiative lifetime in the WL, h and f are the carrier occupation probabilities in the ES and GS, respectively, N_Q is the surface density of QDs, τ_{21} is the electron relaxation time from the ES to the GS, τ_{12} is the electron escape time from the GS to the ES, τ_{1R} is the spontaneous radiative lifetime in the QDs, g is the model gain, and P is the optical power. The electrical field E given by the following equation:

$$\frac{\partial E}{\partial z} = \frac{E}{2}\left[-\alpha + (1 - j\alpha_H) g_{\max}(2f - 1)\right] \quad (4)$$

where α is the loss coefficient, and α_H is the linewidth enhancement factor. The equations for gain G and phase ϕ in the QD-SOAs can be expressed as the following:

$$G = \exp\left\{\sum_{i=1}^{N}\left(g_{\max}(2f-1) - \alpha\right)\left(\frac{L}{N}\right)\right\} \quad (5)$$

$$\frac{\partial \phi_i(z,t)}{\partial z} = -0.5 \times \alpha_H \sum_{i=1}^{N} g_{\max}(2f_i - 1)\left(\frac{L}{N}\right) \quad (6)$$

The equations for the electrical fields E_{out1} and E_{out2} of the output signal from QD-SOA1 and QD-SOA2, respectively, can be expressed as the following:

$$E_{out1} = \frac{E_{in}}{\sqrt{2}}\sqrt{G_1}e^{j(\Delta\phi + \phi_1)} \quad (7)$$

$$E_{out2} = \frac{E_{in}}{\sqrt{2}}\sqrt{G_2}e^{j\phi_2} \quad (8)$$

where, G_1 and G_2 are the gain of QD-SOA1 and QD-SOA2, respectively, ϕ_1 and ϕ_2 are the changed phase values of the QD-SOA1 and QD-SOA2, respectively, and $\Delta\phi$ is the changed phase value of PS. From these equations, the output electrical field E_{out} and the power P_{out} can be expressed as the following:

$$E_{out} = \frac{1}{\sqrt{2}}(E_{out1} - E_{out2}) = \frac{E_{in}}{2}\left(\sqrt{G_1}e^{j(\Delta\phi+\phi_1)} - \sqrt{G_2}e^{j\phi_2}\right) \quad (9)$$

$$P_{out}(t) = |E_{out}|^2 = \frac{P_{in}}{4}\left\{G_1 + G_2 - 2\sqrt{G_1 G_2}\cos[\Delta\phi + \phi_1 - \phi_2]\right\} \quad (10)$$

The first and second terms in Eq. (10) increase as the input signal power increases. However, the third term is cosine-modulated, which increases or decreases as the input signal power increases. Therefore, by adjusting parameters, such as the phase introduced by the PS, the signal power can be increased or decreased even if the first and second terms increase, and the functions of OHL and OPE can realize.

5. Results and Discussion

In this section, we show the performance of the proposed OHL and OPE models connected three OHLs and OPEs. To investigate the performance of the proposed QD-SOA, we numerically solve the rate equations (1)–(3) by using the transfer matrix method [4]. The QD-SOA parameters used in this paper are given in Table 1. Furthermore, we set the additional phase shift $-29°$ for the OHL, and $-43°$ for the OPE. To make a difference in the output signal, the ATT is set at 0 dBm for the proposed OHL, and -5 dBm for the proposed OPE. The signal

Table. 1 Parameters for QD-SOA.

Symbol	Description	Value	Unit
L	effective length of the active layer	2×10^{-3}	m
L_w	effective thickness	0.2×10^{-6}	m
A_{eff}	effective width	2×10^{-6}	m^2
V_g	group velocity	7.859×10^{7}	m/s
q	electron charge	1.602×10^{-19}	C
g_{max1}	maximum modal gain (QD-SOA1)	30×10^{2}	m^{-1}
g_{max2}	maximum modal gain (QD-SOA2) [OHL,OPE]	$[30\times10^{2}, 27\times10^{2}]$	m^{-1}
α_{int}	material absorption coefficient	3.2×10^{2}	m^{-1}
N_Q	surface density of QDs	5×10^{14}	m^{-2}
τ_{w2}	electron relaxation time (WL to ES)	3×10^{-12}	s
τ_{2w}	electron escape time (ES to WL)	1×10^{-9}	s
τ_{wR}	spontaneous radiative lifetime in WL	2×10^{-9}	s
τ_{21}	electron relaxation time (ES to GS)	0.16×10^{-12}	s
τ_{12}	electron escape time from (GS to ES)	1.2×10^{-12}	s
τ_{1R}	spontaneous radiative lifetime	0.4×10^{-9}	s
I	injection current	50	mA
α_{H1}	linewidth enhancement factor (QD-SOA1)	1	-
α_{H2}	linewidth enhancement factor (QD-SOA2)	0.1	-

power input to the OHL is $P_{in} = -7$ dBm, -5 dBm, -3 dBm, -1 dBm, and 0 dBm, respectively, and input to the OPE is $P_{in} = -2$ dBm, -1 dBm, 0 dBm, 1 dBm, 2 dBm, respectively.

We show the input and output waveforms of the proposed OHL model in Fig. 3. The vertical and horizontal axes represent power and time, respectively. Fig. 3(a) shows the input signal waveform. Fig. 3(b) shows the output signal waveform from conventional OHL, and shows that a conventional OHL eliminates the input signal at $P_{in} < -5$ dBm. However, Fig. 3(c) ,which shows output signal waveform from the second OHL, shows that, by using two OHLs, the input signal is eliminated at $P_{in} < -1$ dBm. Also, Fig. 3(d), which shows output signal waveform from third OHL, shows that, by using three OHLs, the output is only $P_{in} = 0$ dBm because the output of the third OHL is relatively well suppressed for $P_{in} < 0$ dBm and is amplified for $P_{in} \geq 0$ dBm.

Fig. 4 shows the input-output characteristics of the proposed OHL and of the conventional model. The vertical axis is the output power which is the peak value of the P_{out} and the horizontal axis is the input power. In Fig. 4, the curves labeled single, double, and triple represent the input-output characteristics of the first, second, and third OHLs, respectively. Fig. 4 shows that the curves tend to be steep for the proposed OHL. The proposed OHL repeats the operation that attenuates the signal whose power is less than the threshold value or amplifies the signal whose power is greater than the threshold value. Therefore, it is possible to make a more significant difference in the output power, and then it has approached to the input-output characteristics of the ideal.

Fig. 5 shows the input and output signal waveforms of the proposed OPE model. Fig. 5(a) shows the input signal waveform; the maximum difference in P_{in} is 4 dBm. Fig. 5(b) shows the output signal waveform from conventional

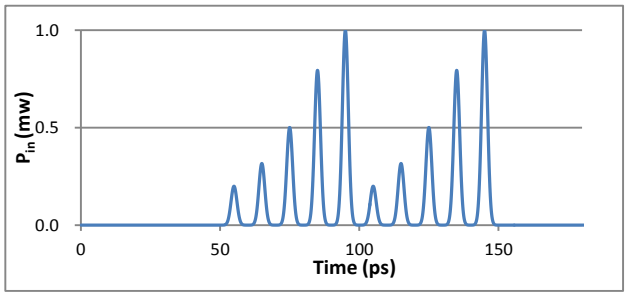

(a) Input signal waveform.

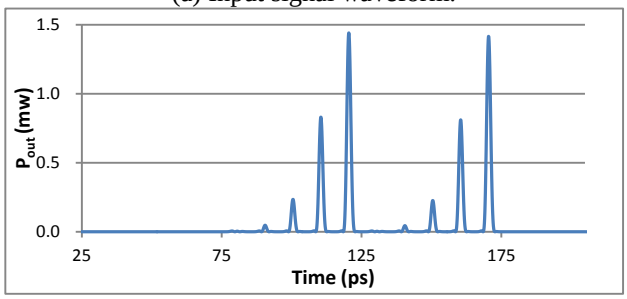

(b) Output signal waveform from conventional OHL.

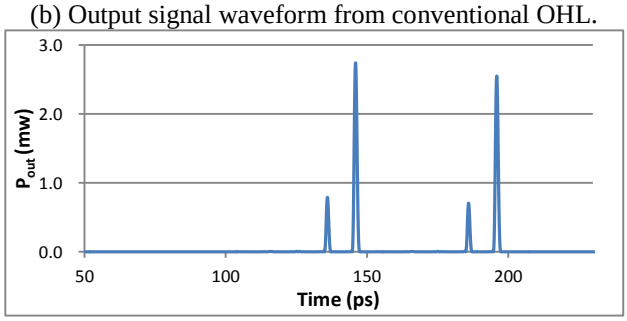

(c) Output signal waveform from the second OHL.

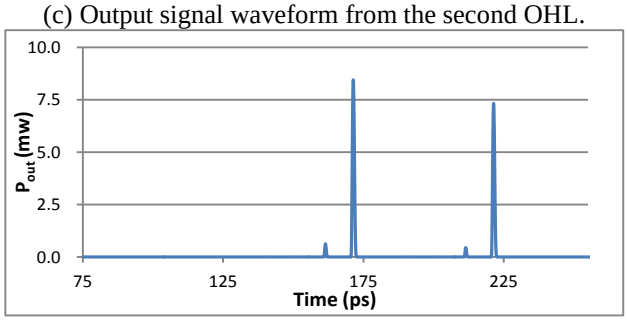

(d) Output signal waveform from third OHL.

Fig. 3 Input signal and output signal for OHL.

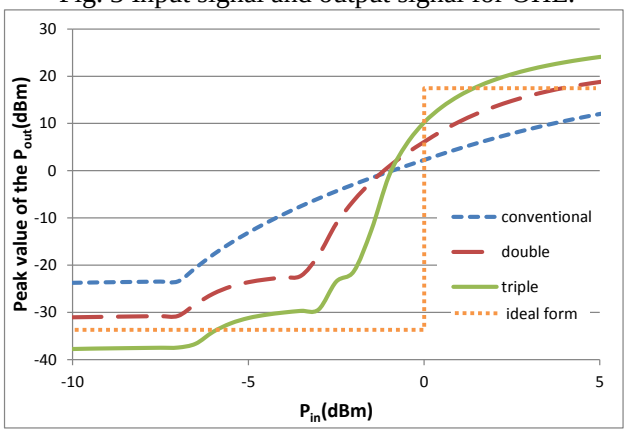

Fig. 4 Input signal vs output signal for OHL.

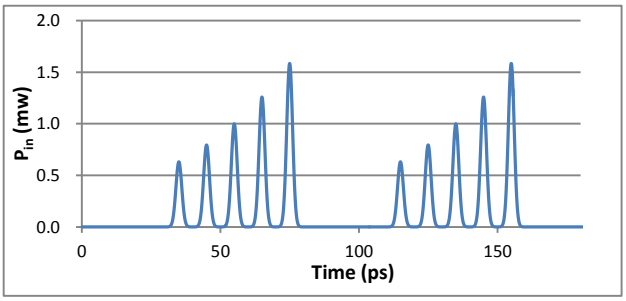

(a) Input signal waveform.

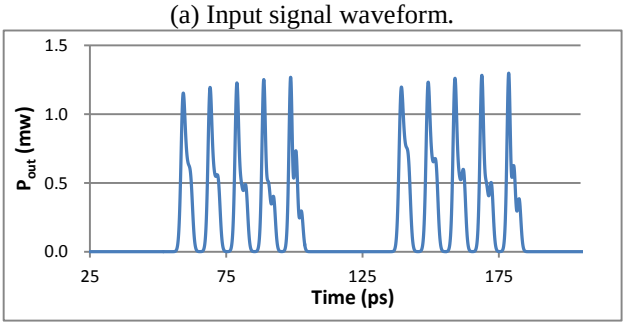

(b) Output signal waveform from conventional OPE.

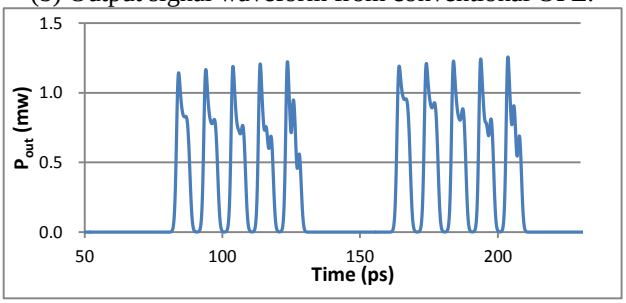

(c) Output signal waveform from second OPE.

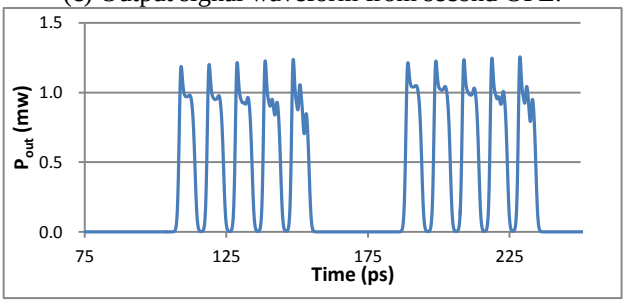

(d) Output signal waveform from third OPE.

Fig. 5 Input signal and output signal for OPE.

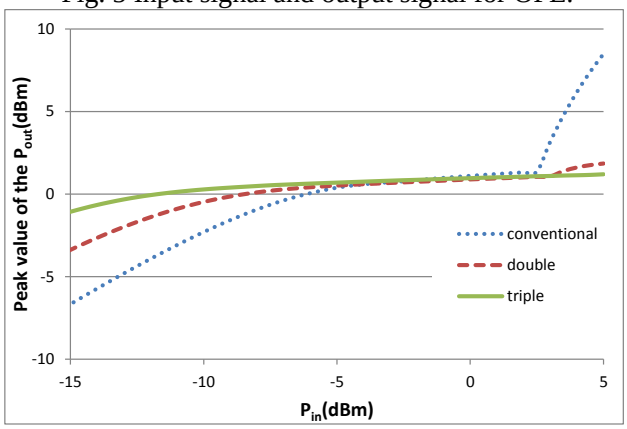

Fig. 6 Input signal vs output signal for OPE.

OPE. It shows that the maximum difference in P_{out} is 0.4 dBm. However, Fig. 5(c) and 5(d), which show output signal waveform from second and third OPE show that, the maximum difference is finally reduced to 0.1 dBm, although the output signal waveform is slightly deformed.

Fig. 6 shows the input-output characteristics of the proposed OHL and of the conventional model. Fig. 6 shows that the range, over which the output power is constant, gradually increases for the proposed OPE, regardless of the input signal power. To describe the output power deviation for an input power ranging from -2 dB to 2 dB, we use 0 dB as the base signal power. The power of the output base signal is P_{outB} and the operating range for the output signal power is $P_{outB} - 0.5$ dBm $< P_{outB} < P_{outB} + 0.5$ dBm. This range results in an operating range of -4.0 to 2.0 dBm for the conventional OPE, -6.5 to 3.0 dBm for the double OPE, and -8.0 to 5.0 dBm for the triple OPE. The results show that the proposed model expands the operating range.

6. Conclusion

We have proposed multiple serially connected OHL and OPE using QD-SOAs, to improve input and output characteristics. By adjusting the output signal power at each stage, it is possible to operate the next OHL and OPE. We numerically analyze the proposed OHL and OPE, and we show that it expands the operating range and improves the input-output characteristics.

Acknowledgments

This research is partly supported by JSPS KAKENHI Grant numbers 25420386 and 25820166.

References

[1] H. Goto, et.al, “All optical intensity equalizer based on effective control of spectral modulation induced by self-phase-modulation using super-Gaussian signals”, ICTON 2008, Vol. 1, pp124-127, Jun.2008.

[2] X. Wu, et.al, “Novel Optical Power Equalizer and Optical Hard Limiter Based on Quantum-Dot Semiconductor Optical Amplifiers”, in Proc. SPIE 7135, Optoelectronic Materials and Devices III, Nov. 2008.

[3] Y.Ben-Ezra, et.al, “Acceleration of Gain Recovery and Dynamics of Electrons in QD-SOA”, IEEE JORUNAL OF QUANTUM ELECTRONICS, VOL.41, NO.10, pp1268-1273, Oct. 2005.

[4] H.Lee, et.al, “Theoretical Study of Frequency Chirping and Extinction Ratio of Wavelength-Converted Optical Signals by XGM and XPM Using SOA’s”, IEEE JORUNAL OF ELECTRONICS, VOL.35, No.8, pp1213-1219, Aug. 1999.

[5] Y.Ben-Ezra, et.al, “Ultrafast All-Optical Processor Based on Quantum-Dot Semiconductor Optical Amplifiers”, IEEE JORUNAL OF QUANTUM ELECTRONICS, VOL.45, NO.1, pp34-41, Jan. 2009.